https://doi.org/10.31436/iiumej.v26i2.3463

DESIGN AND OPTIMIZATION OF A FLEXIBLE ANTENNA FOR ISM BAND WEARABLE DEVICES VIA INSET SLOT INTEGRATION AND PARASITIC ELEMENTS

AIMAN HAKIMI RAHIMI, SARAH YASMIN MOHAMAD*, NORUN FARIHAH ABDUL MALEK, FARAH NADIA MOHD ISA, AHMAD ZAMANI JUSOH, AISHA HASSAN ABDALLA HASHIM

Microwave, Communication and Information Systems Engineering (MCISE) Research Group, Department of Electrical and Computer Engineering, Kulliyyah of Engineering, International Islamic University Malaysia, Kuala Lumpur, Malaysia

**Corresponding author: smohamad@iium.edu.my*

(Received: 4 October 2024; Accepted: 13 January 2025; Published online: 15 May 2025)

ABSTRACT: This paper aims to analyze and optimize the electrical properties of a flexible antenna to maximize its potential. The antenna's performance is enhanced by incorporating inset slots on both the patch and ground plane, as well as utilizing parasitic elements to improve the resonant frequency and achieve a wider bandwidth. The flexible antenna is designed to resonate within the Industrial, Scientific, and Medical (ISM) frequency band of 5.725–5.875 GHz, using Rogers RO4003C with a dielectric constant of 3.55 and dimensions of 20 × 25 × 0.2032 mm³. The proposed antenna demonstrates promising results, with S_{11} of -37.05 dB at 5.78 GHz, and a bandwidth of 158 MHz, ranging from 5.739–5.897 GHz. The usable ISM bandwidth is 136 MHz, representing 90.67% of the ISM frequency band. Theoretical, simulation, and experimental analyses confirm that embedding slots on the patch or ground plane, along with the use of parasitic elements, significantly enhances the antenna's resonant frequency, bandwidth, and efficiency. Because of its flexibility, improved resonant frequency, and wide bandwidth, this antenna has potential uses in the ISM frequency band to enable faster and more efficient data transmission.

ABSTRAK: Kajian ini bertujuan bagi menganalisa dan mengoptimum sifat elektrik antena fleksibel bagi memaksimum potensinya. Ciri-ciri antena dipertingkatkan lagi dengan penggunaan slot sisipan pada tampalan dan satah tanah, dan menggunakan elemen parasitik bagi meningkatkan frekuensi resonan dan mencapai lebar jalur yang lebih luas. Antena fleksibel ini direka untuk frekuensi Industri, Saintifik dan Perubatan (ISM) iaitu pada frekuensi 5.725–5.875 GHz menggunakan Rogers RO4003C dengan pemalar dielektrik 3.55 dan dimensi 20 × 25 × 0.2032 mm³. Antena yang dicadangkan ini menunjukkan hasil yang baik dengan S_{11} -37.05 dB pada frekuensi 5.78 GHz, dan jalur lebar 158 MHz, dalam julat 5.739–5.897 GHz. Jalur lebar ISM mencapai 136 MHz iaitu bersamaan 90.67% jalur frekuensi ISM. Analisis teori, simulasi dan eksperimen membuktikan bahawa penggunaan slot pada tampalan atau di atas satah tanah, bersama elemen parasitik dapat membantu meningkatkan frekuensi resonan, lebar jalur dan kecekapan antena. Oleh kerana fleksibilitinya, frekuensi resonan meningkat dan jalur lebar bertambah luas. Antena ini berpotensi bagi penggunaan jalur frekuensi ISM dengan penghantaran data yang lebih pantas dan cekap.

KEYWORDS: *Flexible microstrip antenna, inset slots, parasitic elements, Industrial, Scientific, and Medical (ISM) band.*

https://doi.org/10.31436/iiumej.v26i2.3463

1. INTRODUCTION

Modern communication networks have seen substantial advancements in system development, driven by technological integration and innovation. Among the critical components in communication technology, antennas stand out for their reliability. However, traditional antennas, with their rigid and fragile structures, often lack the durability and flexibility required for specific applications [1,2]. In contrast, flexible antennas, which rely heavily on the substrate material, are crucial to the functionality of contemporary communication systems. A variety of materials have been researched, tested, and employed in the development of flexible antennas, including rubber [3], polydimethylsiloxane (PDMS) [4–5], polyethylene terephthalate (PET), thermoplastic polyurethane, and elastomers (TPU and TPE) [6], and Rogers RO4003C [7]. These materials provide flexible antennas with excellent elasticity, stable electrical properties, and the added benefits of being lightweight and low profile, making them more adaptable compared to traditional antennas mounted on rigid substrates. For wearable applications, the antenna must be physically flexible, capable of conforming to the body, especially since it involves integrating with the body on uneven surfaces, as shown in Figure 1 [8].

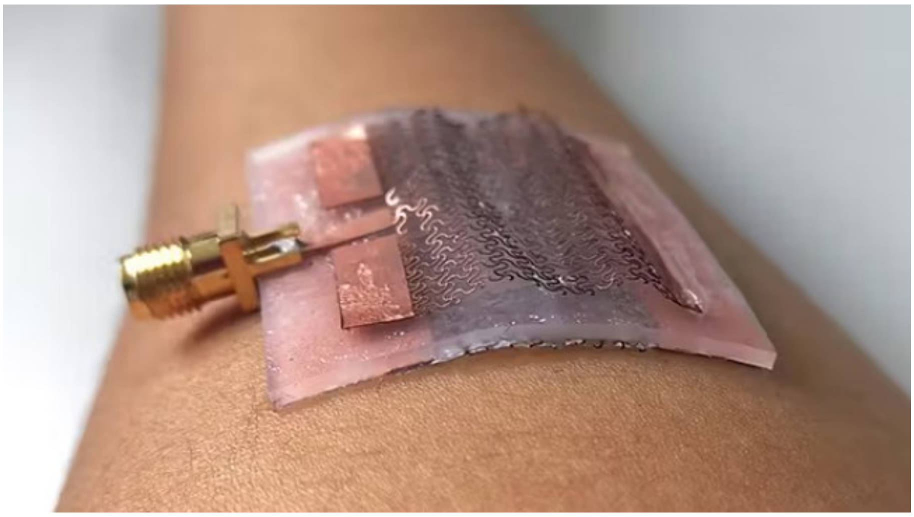

Figure 1. On-body flexible antenna [8].

According to [9], wearable antennas are highly versatile, capable of achieving multiband designs and characteristics suited for various applications, including the ISM band, C-band, Bluetooth, Worldwide Interoperability for Microwave Access (WiMAX), 5G smartphones, radio altimeters, and satellite TV. While several flexible antennas have been developed, many do not operate within the ISM band, lack multiband functionality, or do not provide wideband performance.

Wireless applications greatly benefit from antennas that offer both flexibility and broad bandwidth. A wider bandwidth is particularly advantageous for wireless networking, allowing for better utilization of the designated frequency spectrum. Over the past decade, the adoption of broadband technology has grown substantially due to its numerous advantages, including enhanced communication security, higher data transfer rates, improved power efficiency, reduced signal interference, optimized spectrum utilization, and simplified circuitry.

Several techniques have been used to enhance the bandwidth of microstrip antennas, including the use of inset slots on the patch [10–11], the introduction of parasitic elements [12], and modifications to the ground plane [13]. In [10], the authors employed slots and an inset feed to improve impedance matching, gain, and return loss for Wireless Body Area Network (WBAN) applications. Antenna design plays a crucial role in WBAN, as comfort and reliability directly influence antenna efficiency. Polyimide was selected as the substrate due to its flexibility and low dielectric constant, which minimizes surface wave losses, making it ideal for this application. Proper feeding techniques were used to control impedance matching and return loss, which in turn affect various antenna performance parameters.

In [12], U-shaped slotted antennas have gained popularity in antenna design due to their ability to improve performance, particularly in terms of gain. The U-slot extends the current path, allowing for current perturbation that generates circular polarization. The inclusion of parasitic elements, positioned beside the central patch, further enhances the antenna's bandwidth by acting as additional radiators. The authors also integrated parasitic elements in a single-layer patch, along with slots, to boost bandwidth, gain, and efficiency for applications such as Wireless Gigabit (WiGig) and Wireless Personal Area Network (WPAN). Additionally, modifications to the ground plane have been implemented to enhance impedance bandwidth [13]. Ground plane alterations, such as inserting slots and using metamaterials, have been widely accepted by researchers as they significantly contribute to generating multiband frequencies.

Moreover, the laminating manufacturing technique employed for the single-patch and Multiple Input Multiple Output (MIMO) textile antenna in [14] enhances the reproducibility of textile antennas. The MIMO system, which utilizes multiple transmitters and receivers, improves performance, reliability, and coverage. This system is designed for fifth-generation (5G) on-body applications, further advancing IoT development and extending 5G frequencies to cover the ISM band at 5.8 GHz. Traditional manufacturing processes often introduce inaccuracies, such as frequency shifts, that can negatively impact antenna performance.

All these studies demonstrate that adding slots improves both resonant frequency and return loss, while parasitic elements contribute to broader bandwidth. Ground plane modifications increase parasitic capacitance in the fringing field due to a defective ground structure, thereby enhancing the coupling between the ground plane and the patch, ultimately resulting in increased bandwidth.

In this paper, we present methods to enhance the bandwidth and performance of a flexible microstrip antenna operating within the ISM frequency band range of 5.725–5.875 GHz. The antenna design includes a coplanar waveguide (CPW) technique, parasitic elements, and inset slots on both the patch and ground plane. The inset slots on the patch are expected to improve resonant frequency and return loss by extending the surface current paths of the resonant modes, thus lowering the corresponding resonant frequencies. Moreover, including parasitic elements enhances antenna efficiency and broadens the bandwidth. The design methodology and computations, based on fundamental equations, are detailed in Section 2. Section 3 presents an analysis of the simulation and experimental results, focusing on key performance metrics such as return loss, bandwidth, directivity, efficiency, VSWR, and radiation pattern. The optimized antenna, utilizing the flexible Rogers RO4003C substrate, demonstrated a return loss of -37.05 dB and a wide bandwidth of 158 MHz (5.739–5.897 GHz). Within the 5.725–5.875 GHz ISM frequency band, the antenna achieved a bandwidth of 136 MHz. We also present the antenna's performance under 45° bending conditions, with both simulated and measured results demonstrating acceptable performance. Despite frequency shifts, the antenna maintains reliable functionality thanks to its wide bandwidth.

https://doi.org/10.31436/iiumej.v26i2.3463

2. METHODOLOGY

2.1. Antenna Equations

The proposed antenna was designed, simulated, and analyzed using Computer Simulation Technology Microwave Studio (CST MWS) software. Based on calculations derived from the fundamental equation for a basic rectangular patch antenna, a rectangular patch antenna targeting an operating frequency of 5.78 GHz (the center of the 5.725–5.875 GHz ISM band) was developed.

Three key factors were considered to determine the patch dimensions and ensure proper impedance matching between the radiating patch and the transmission line: the selected material's resonant frequency, dielectric thickness, and dielectric constant. For this design, the Rogers RO4003C substrate was chosen for its flexibility and favorable characteristics, including a dielectric constant of 3.55, a thickness of 0.2032 mm, and a dielectric strength of 780 V/mil. The specified values of the operating frequency (f_o), substrate thickness (h) and substrate relative permittivity of the dielectric constant (ε_r) are applied accordingly to define the computational value of patch width (W_p) and patch length (L_p). The patch width (W_p) is calculated as in Eq. (1).

$$W_p = \frac{c}{2f_o\sqrt{\frac{(\varepsilon_r+1)}{2}}} \tag{1}$$

Where c is the speed of light, 3×10^8 m/s. The effective dielectric constant (ε_{eff}) is calculated using Eq. (2), which is based on the substrate height, dielectric constant, and calculated patch width in Eq. (1).

$$\varepsilon_{eff} = \frac{\varepsilon_r+1}{2} + \frac{\varepsilon_r-1}{2}\left[1 + 12\frac{h}{W_p}\right]^{-\frac{1}{2}} \tag{2}$$

The patch length (L_p) is calculated using Eq. (3), which involves the difference between effective length (L_{eff}) and length extension (ΔL), calculated using Eqs. (4) and (5) respectively.

$$L_p = L_{eff} - 2\Delta L \tag{3}$$

$$L_{eff} = \frac{c}{2f_o\sqrt{\varepsilon_{eff}}} \tag{4}$$

$$\Delta L = 0.412h\frac{(\varepsilon_{eff}+0.3)\left(\frac{W_p}{h}+0.264\right)}{(\varepsilon_{eff}-0.258)\left(\frac{W_p}{h}+0.8\right)} \tag{5}$$

The feedline width (W_f) is determined using macros in CST features, which calculate the analytical line impedance to achieve a suitable width for good impedance matching of 50Ω between the feedline and the antenna radiating patch. Moreover, the feedline width can be calculated using Eq. (6), where Z_o represents the input impedance. Securing impedance matching is essential to ensure that power can be supplied without having losses, leading to improved accuracy in antenna performance.

$$W_f = \frac{7.48h}{e^{\left(Z_o\sqrt{\frac{(\varepsilon_r+1.41)}{87}}\right)}} - 1.25t \tag{6}$$

Applying these equations and optimizing the dimensions obtained a patch width of 18.53 mm and a length of 13.81 mm.

2.2. Optimization and Finalized Dimensions

Figure 2 illustrates the antenna dimensions before optimization, derived from the equations in Section 2.1. Several modifications were applied to the initial patch design to achieve the desired resonant frequency of 5.78 GHz and enhance overall performance. These included the introduction of an inset feedline (Figure 3a), the addition of slots on both the patch (Figure 3b–c) and ground plane (Figure 3d), the integration of two parasitic elements (Figure 3e), and the incorporation of cutting edges on the patch antenna (Figure 3f).

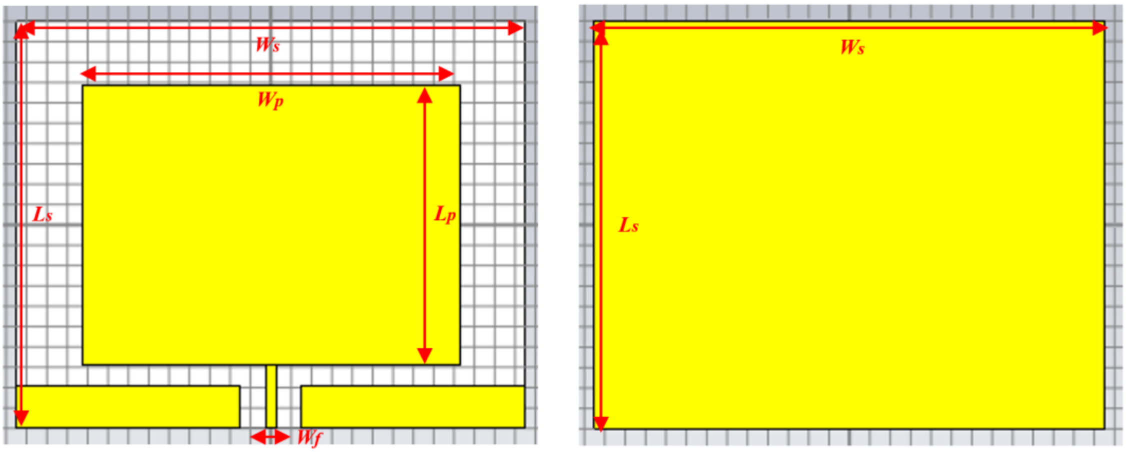

(a) Top View (b) Bottom View

Figure 2. Initial antenna dimensions before optimization.

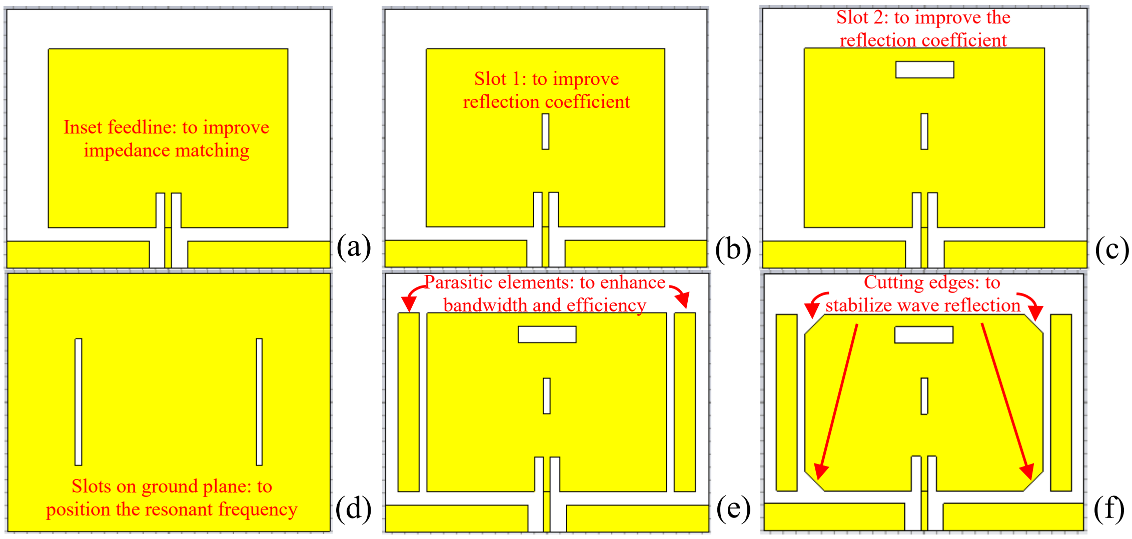

Figure 3. Optimization stages of the proposed antenna: (a) inset feedline, (b) slot 1 on patch, (c) slot 2 on patch, (d) slots on ground plane, (e) parasitic elements, and (f) cutting edges.

To address the limited bandwidth of a standard rectangular patch antenna, the feedline is designed with a coplanar waveguide (CPW), incorporating ground plane elements. The process begins with introducing an inset feedline, as shown in Figure 3a, to ensure impedance matching between the radiating patch and the feedline. Subsequently, slots are introduced to the patch and the ground plane to improve reflection coefficient performance and enhance overall efficiency, as depicted in Figure 3 b–d. Previous studies [9] have demonstrated that introducing a slot into the antenna structure can extend the surface current paths of the resonant modes, thereby lowering the corresponding resonant frequencies and improving both resonance and return loss. In implementing the CPW technique, a partial ground plane near the feedline creates gaps of 1 mm and 1.25 mm between the radiating patch and the feedline, respectively.

Additionally, two parasitic elements are positioned on the left and right sides of the radiating patch, as shown in Figure 3e, with gaps of 1 mm and 0.6 mm from the patch edge and the radiating patch, respectively. This parasitic element technique enhances bandwidth and improves antenna efficiency, as demonstrated in [13]. The cutting-edge design of the patch, depicted in Figure 3f, further stabilizes the antenna by minimizing wave reflection.

The final design was implemented on a 20 × 25 × 0.2032 mm^3 Rogers RO4003C substrate, as shown in Figure 4. The dimensions of the proposed antenna are detailed in Table 1, which includes parameters such as substrate width (W_s), substrate length (L_s), substrate thickness (h), patch width (W_p), patch length (L_p), patch thickness (t), feedline width (W_f), multiple slots consisting of inset slot (si), slot 1 ($s1$), slot 2 ($s2$) and back slot (sb).

Table 1. Finalized dimensions of the proposed antenna as in Figure 4.

Parameter	mm	Parameter	mm	Parameter	mm	Parameter	mm
W_s	25	W_p	18.53	W_{si}	0.7	W_{s2}	4.5076
L_s	20	L_p	13.81	L_{si}	2.7	L_{s2}	1.25
h	0.2032	t	0.035	W_{s1}	0.5076	W_{sb}	0.5
W_f	0.5076			L_{s1}	2.81	L_{sb}	9.81

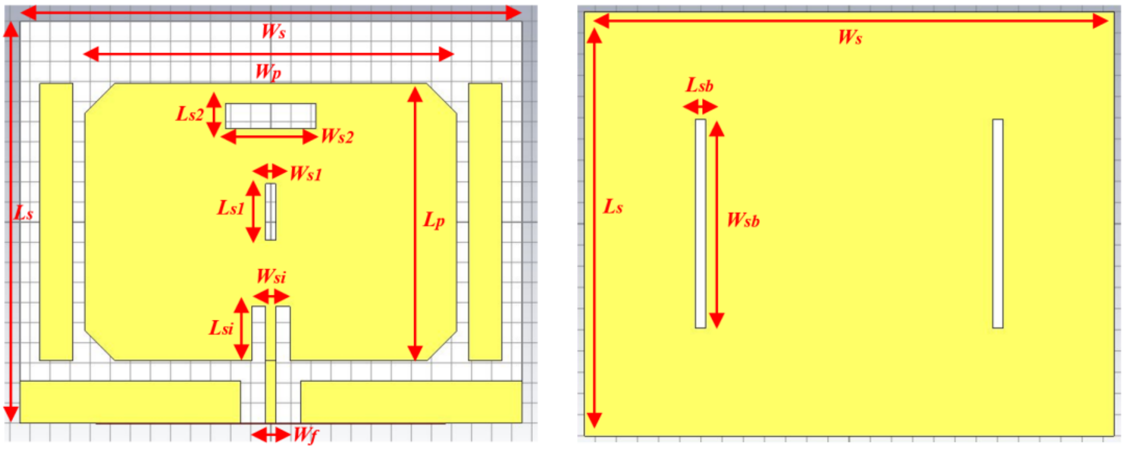

(a) Top View (b) Bottom View

Figure 4. Finalized antenna dimensions after optimization with inset slots, parasitic elements, and cutting edges.

3. RESULTS AND DISCUSSION

The antenna's performance was evaluated in terms of return loss, bandwidth, directivity, efficiency, VSWR, and radiation pattern. The simulated return loss and bandwidth are presented in Figure 5. After optimization, the antenna achieved a resonant frequency at the center of the ISM band, with a return loss of -37.05 dB at 5.78 GHz (red curve), a significant improvement over the pre-optimization value of only -2.74 dB (green curve), which was inadequate for proper operation. Adding inset slots on both the patch and the ground plane (Figure 3 b–d) greatly enhanced the antenna's performance, precisely controlling the targeted frequency band. These slots contributed to improved bandwidth and efficiency, while extending the slot length on the ground plane shifted the resonant frequency to a lower range, effectively reducing the antenna size.

Furthermore, the antenna resonated within the usable frequency range of 5.739–5.897 GHz, meeting the -10 dB threshold and resulting in a bandwidth of 158 MHz, as depicted in Figure 5. This bandwidth effectively covers 136 MHz, corresponding to 90.67% of the 5.725–5.875 GHz ISM band. In the design, the parasitic elements positioned beside the central patch (Figure 3e) are electrically isolated from it but are inductively coupled, facilitating energy transfer to and from the central patch. This inductive coupling influences the antenna's impedance, generating an additional resonant frequency close to the original. While the resonant frequency produced by the parasitic elements is weaker than the primary frequency, the key objective of this technique is to broaden the antenna's bandwidth. This method has proven effective in significantly enhancing the overall bandwidth.

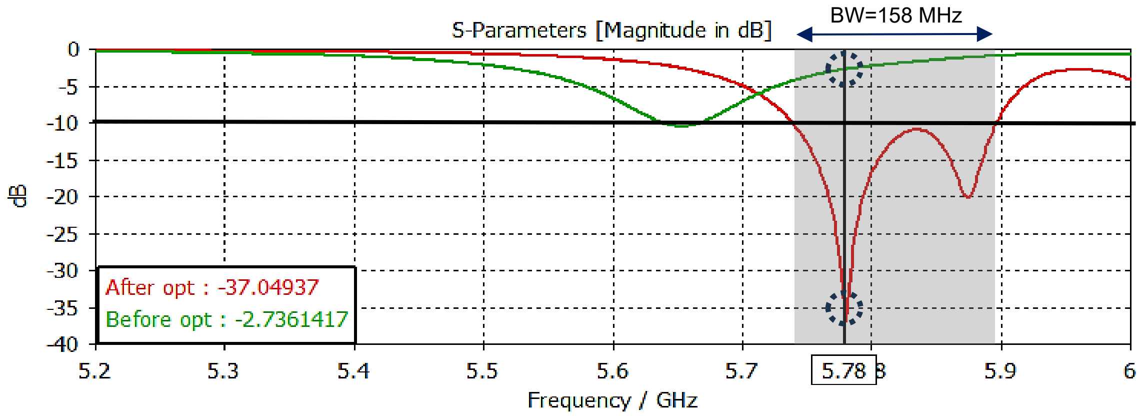

Figure 5. Simulated return loss S_{11} and bandwidth of the proposed antenna at 5.78 GHz before and after optimization.

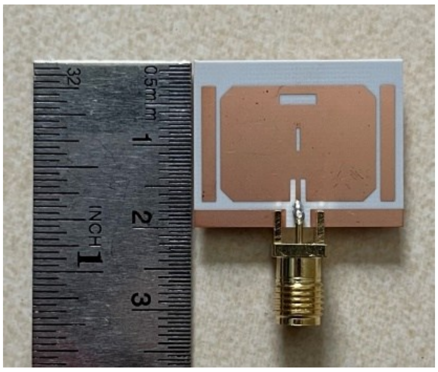

(a) Top View

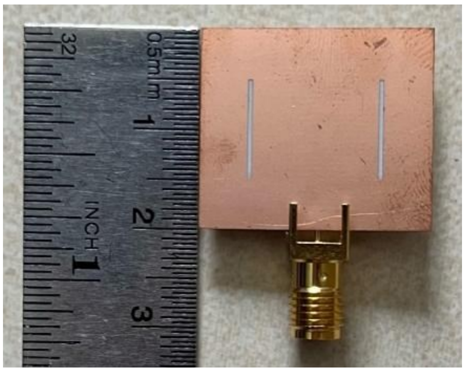

(b) Bottom View

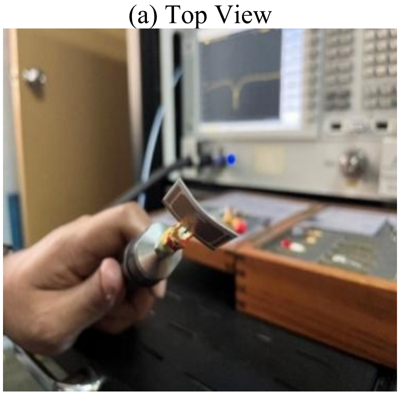

(c) Antenna Under Test using VNA

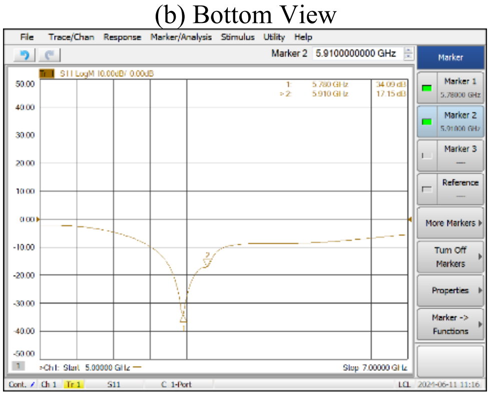

(d) Measured Return Loss

Figure 6. Fabricated antenna.

The prototype displayed in Figure 6a–b showcases the fabricated antenna, which has overall dimensions of 20 × 25 × 0.2032 mm³. The antenna's performance was evaluated using a Vector Network Analyzer (VNA) to obtain the actual return loss results, as illustrated in Figure 6c–d.

Figure 7 compares the simulated (red curves) and measured (blue curves) return loss of the microstrip patch antenna used in this study, showing strong agreement between the two sets of results. The antenna showed a measured return loss of -35.24 dB at 5.78 GHz, with a usable frequency range of 5.6–6.0 GHz. The return loss measurements closely matched the simulations, showing two resonant frequencies in both datasets. The flexibility and electrical properties of the chosen substrate helped achieve a better measured return loss, resulting in a bandwidth of 400 MHz, over twice that of the simulated return loss. Therefore, the antenna effectively covered a frequency range of 150 MHz, corresponding to 100% of the 5.725–5.875 GHz ISM frequency band.

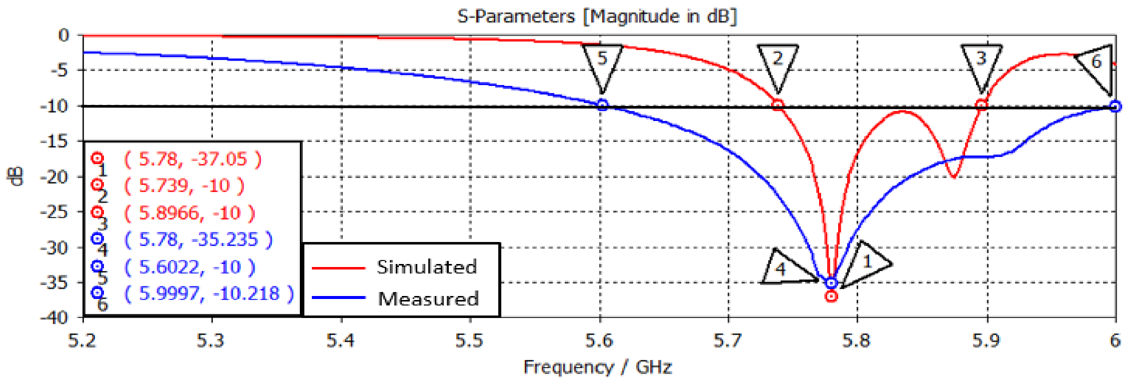

Figure 7. Simulated and measured return loss (S_{11}) under flat conditions at 5.78 GHz.

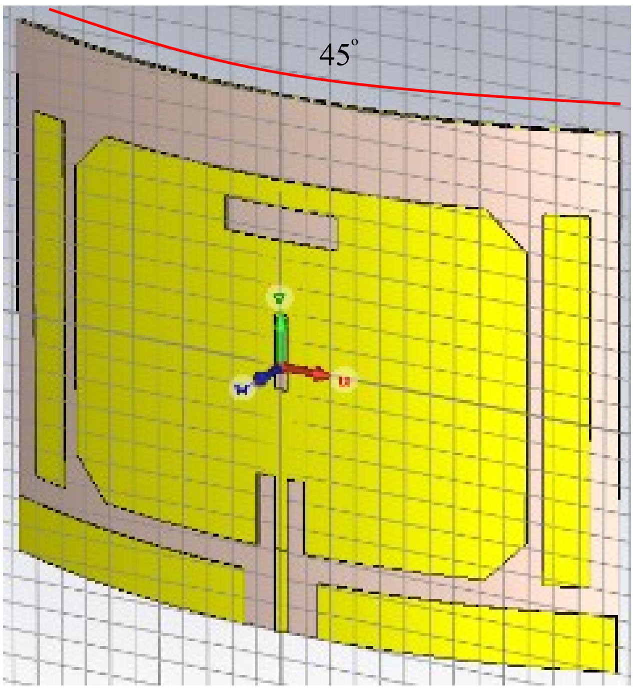

Figure 8. Antenna on 45° bend curvature in CST.

https://doi.org/10.31436/iiumej.v26i2.3463

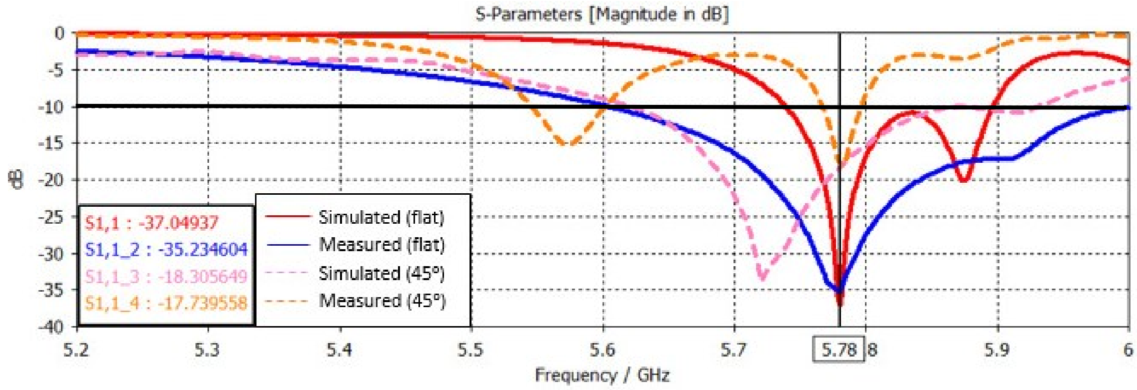

Figure 9. Simulated and measured return loss of the antenna under flat conditions and 45° bending state at 5.78 GHz.

In addition to analyzing the antenna in a flat condition, the bending of the flexible antenna was also simulated and examined. Demonstrating the antenna's flexibility is essential for wearable applications to ensure that the antenna can work efficiently in both flat and bent conditions. The microstrip patch antenna was simulated at a bending curvature of 45° (Figure 8). Bending significantly affects the flexible antenna's return loss, leading to signal strength variations due to impedance mismatches with the feedline and the influence of surface waves. As a result, signal strength increases while the resonant frequencies shift to lower values (Figure 9). These findings indicate a notable improvement in signal strength and underscore impedance mismatch as the most significantly impacted factor in this context.

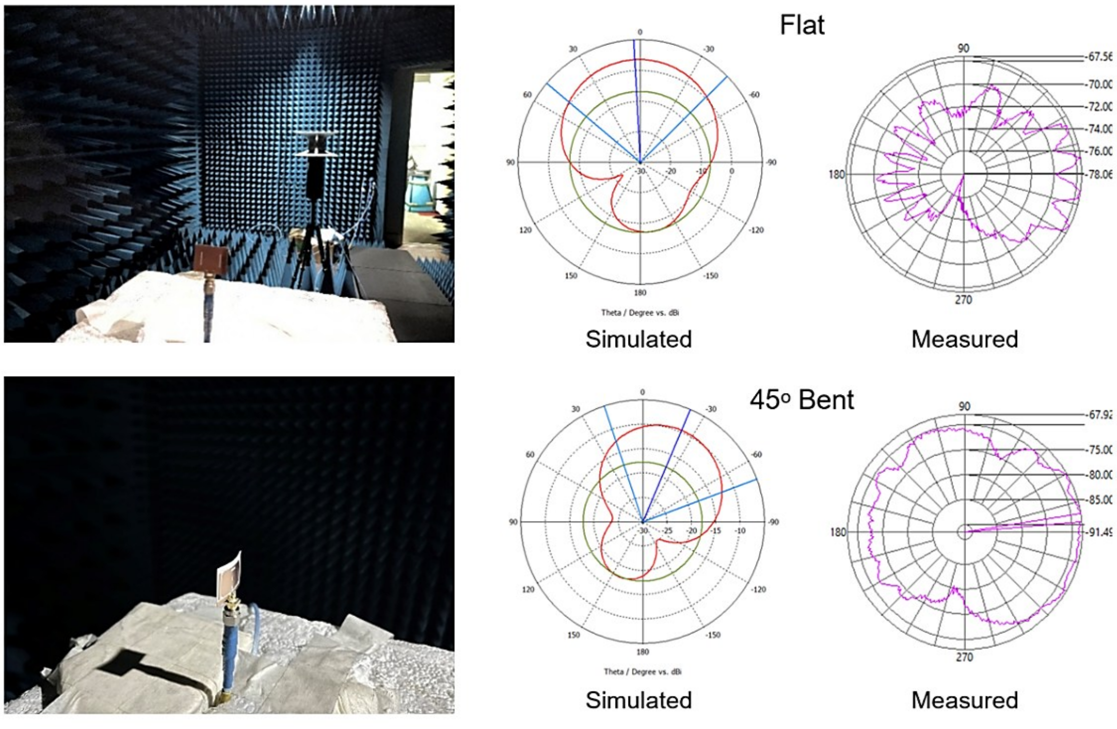

(a) (b)

Figure 10. (a) Antenna measurement in anechoic chamber under flat and 45° bent state, (b) simulated and measured antenna pattern at 5.78 GHz under flat and 45° bent state

https://doi.org/10.31436/iiumej.v26i2.3463

The measurement setup for the antenna within an anechoic chamber, along with the polar pattern of the antenna, is presented in Figure 10a and Figure 10b, respectively. The microstrip patch antenna was placed on a custom 45° carved Styrofoam to justify the angle and ensure it can be precisely adjusted. Then, the bending is done carefully by tilting the antenna to the desired 45° angle using a mechanical tool. It is essential to ensure that the bending does not damage the antenna structure, especially on the substrate. Once the antenna is bent, it is secured in the bending position for a significant amount before it reverts to its original state. This procedure effectively allows the antenna to be measured in the anechoic chamber to achieve the highest efficiency possible. The antenna demonstrates a directional radiation pattern, which enables effective operation within the specified frequency range. The advanced patch design facilitates circular polarization with an axial ratio of 2.54, allowing the antenna to receive power from any incident wave angle consistently. Practical circularly polarized antennas typically have values of 1 to 3 in many real-world scenarios. The closer the axial ratio is to 1, the better the circular polarization. When slots are introduced on the ground plane (Figure 3d), the electric field influences the radiation pattern, behaving as a magnetic dipole. The E-plane radiation pattern experiences some changes due to diffraction effects resulting from the edges of the finite-sized ground plane.

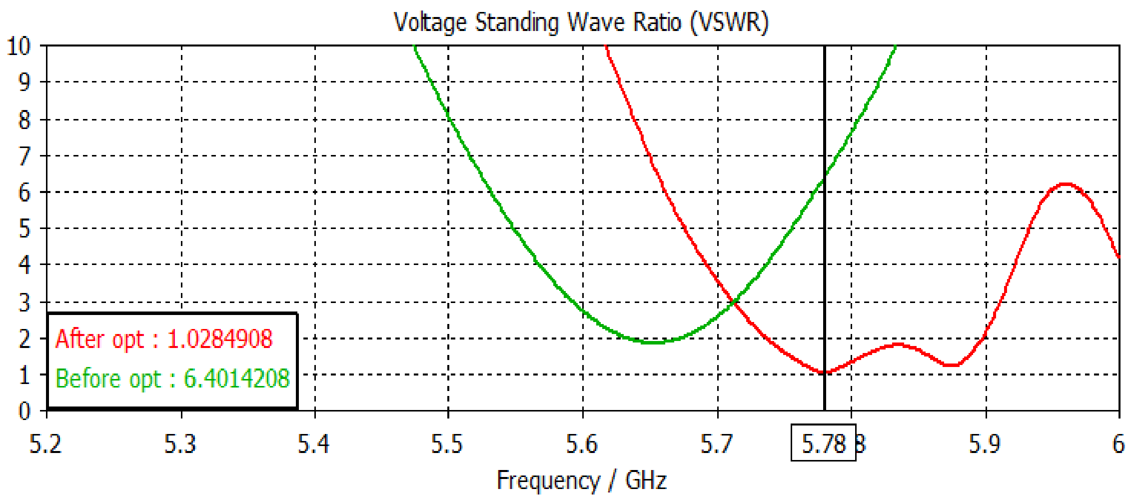

(a) Before and after optimization

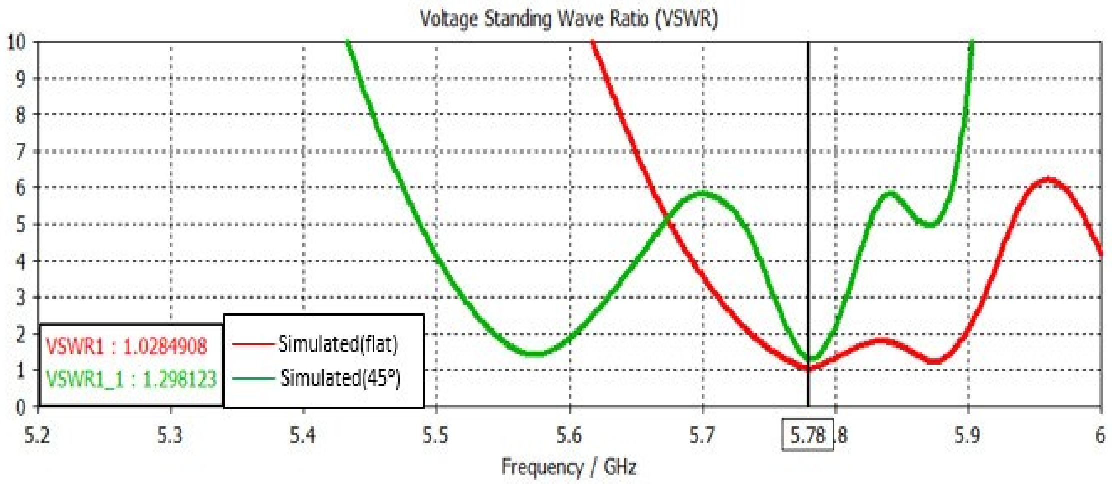

(b) Under flat and bending state of 45°

Figure 11. Simulated VSWR of the proposed antenna at 5.78 GHz.

https://doi.org/10.31436/iiumej.v26i2.3463

The radiation patterns of the antenna exhibit similar characteristics under both simulated and measured conditions in a flat configuration. However, the measured pattern under a 45° bend condition shows slight deviations from the simulated pattern due to the effects on the surface current wave. The variability in the measured patterns is likely caused by cable attenuation, which can lead to unavoidable signal distortion. Nonetheless, these observations are acceptable as they reflect the realistic conditions considered in this analysis. The antenna demonstrates a directivity of 6.26 dBi at 5.78 GHz, resulting in an antenna efficiency of 55.65%. This performance is considered satisfactory for a single radiating patch antenna. Under bending conditions, the directivity decreased to 4.29 dBi with corresponding efficiencies of 52.86% at 45° bending. However, the overall performance could be enhanced in future work by applying various modification principles related to the microstrip patch antenna design.

The Voltage Standing Wave Ratio (VSWR) fundamentally measures the degree of mismatch between an antenna and its connecting feedline. After optimization with slots and parasitic elements, the proposed antenna recorded an acceptable VSWR of 1.03, while the high VSWR of 6.44 observed prior to optimization is not ideal for patch antennas, as illustrated in Figure 11a. The effects of bending on VSWR are also depicted in Figure 11b, which shows that the VSWR remains stable even after bending, with a VSWR of 1.3 (45° bent).

Table 2 summarizes the performance of the flexible microstrip patch antenna in terms of S_{11} (dB), usable and ISM bandwidth (MHz), directivity (dBi), efficiency (%), and VSWR, before and after optimization. At 5.78 GHz, the antenna exhibits excellent performance with a simulated and measured return loss of -37.05 dB and -35.24 dB, respectively. The antenna exhibits a usable bandwidth of 158 MHz (5.739–5.897 GHz), and an ISM bandwidth of 136 MHz. The antenna also produced a directivity of 6.26 dBi, an efficiency of 55.65%, and a VSWR of 1.03.

Table 2. Antenna performances in terms of S_{11}, usable bandwidth, ISM bandwidth, directivity, efficiency, and VSWR before and after optimization in flat and 45° bend conditions at 5.78 GHz.

Parameters	Flat Before OPT	Flat After OPT	Bent (45°) After OPT	Value Improvement Flat Before vs. After OPT
S_{11} (dB)	-2.74	-37.05 (sim) -35.24 (mea)	-18.31 (sim) -17.74 (mea)	34.31 dB
Usable Bandwidth (MHz)	0	158 (sim) 400 (mea)	260 (sim) 29 (mea)	158 MHz
ISM Bandwidth (MHz)	0	136 (sim) 150 (mea)	150 (sim) 29 (mea)	136 MHz
Directivity (dBi)	6.39	6.26	4.29	-0.13 dBi
Efficiency (%)	1.75	55.65	52.86	53.9%
VSWR	6.40	1.03	1.30	5.37

*OPT = optimized, sim = simulation, mea = measurement.

Following a 45° bend, the antenna continues to perform effectively, with an S_{11} value of -18.31 dB (measured -17.74 dB). It is well known that bending can impact antenna performance, particularly by causing frequency shifts, underscoring the importance of a wide bandwidth to maintain functionality at the target frequency. While directivity and efficiency are slightly reduced to 4.29 dBi and 52.86%, respectively, these values remain within acceptable limits. Additionally, the VSWR remains below 2, with a 1.30 value indicating stable performance.

Table 3 compares the proposed antenna in this work with other ISM antennas available in the literature, operating within the frequency range of approximately 5.725–5.875 GHz. This includes a variety of different flexible materials such as FR4 [15–16], Rogers RT5880 [17–19], jeans [20], and polyimide [21]. Our antenna exhibits commendable performance within the ISM frequency band with enhanced S_{11}, bandwidth, and VSWR while maintaining reliable functionality under bending conditions. These results imply that the suggested antenna would be a good option for various ISM band applications that require a flexible structure and a wide bandwidth.

Table 3. Comparison of the proposed antenna with other latest flexible ISM antennas found in the literature [15–21] in terms of dielectric constant, flexibility, S_{11}, usable bandwidth, VSWR, bending study, and experimental analysis.

Ref	Substrate	Freq (GHz)	ε_r	Flexibility	S_{11} (dB)	BW (MHz)	VSWR	Bending study	Fabricated & measured
[15]	FR4	5.80	4.40	No	-18.32	150	1.5	No	NR
[16]	FR4	5.80	4.40	No	-20.59	315	NR	No	Yes
[17]	RT5880	5.80	2.20	No	-13.75	NR	NR	No	No
[18]	RT5880	5.80	2.20	No	-39.30	NR	1.6	No	No
[19]	RT5880	5.80	2.20	No	-13.90	NR	1.01	No	No
[20]	Jeans	5.80	NR	Yes	-31.72	NR	1.73	No	No
[21]	Polyimide	5.70	3.50	Yes	-25.00	150	NR	Yes	Yes
Proposed antenna	**RO4003C**	**5.78**	**3.55**	**Yes**	**-37.05**	**158**	**1.03**	**Yes**	**Yes**

*NR = not reported, Freq = frequency, ε_r = dielectric constant, BW = bandwidth.

4. CONCLUSIONS

A flexible microstrip patch antenna with a coplanar waveguide (CPW) has been proposed for the 5.725–5.875 GHz ISM frequency band. The antenna is designed to resonate at 5.78 GHz on 8 mil (0.2032 mm) RO4003C material, with optimized dimensions of 20 × 25 × 0.2032 mm³. It was simulated using CST Microwave Studio (CST MWS) software and measured with a Vector Network Analyzer (VNA) to assess return loss, and with an anechoic chamber to assess the radiation pattern. Incorporating inset slots on the patch, feedline, and ground plane, along with the addition of parasitic elements adjacent to the central patch, has led to significant improvements in the antenna's performance, particularly in enhanced resonant frequency and wider bandwidth. The inset slots improve the reflection coefficient, while the parasitic element technique amplifies bandwidth and increases antenna efficiency. The achieved usable bandwidth is 158 MHz and an ISM bandwidth of 136 MHz, corresponding to 90.67% of the 5.725–5.875 GHz ISM frequency band. Additionally, the return loss performance of the antenna has improved remarkably from -2.74 dB to -37.05 dB, exhibiting acceptable directivity compared to conventional methods for designing standard patch antennas. Apart from that, the antenna was also analyzed under 45^{o} bending, demonstrating the flexibility and satisfactory performance of the proposed antenna, which can benefit wearable applications. This antenna has potential applications in the ISM frequency band, such as in smartwatch technology and wireless body-area network (WBAN) applications, to facilitate faster and more efficient data transmission due to its flexibility, enhanced resonant frequency, and large bandwidth.

ACKNOWLEDGEMENTS

This research was supported by the International Islamic University Malaysia (IIUM) and the Ministry of Higher Education Malaysia (MOHE) through the Fundamental Research Grant Scheme FRGS/1/2023/TK07/UIAM/02/1.

REFERENCES

[1] Kirtania SG, Elger AW, Hasan MR, Wisniewska A, Sekhar K, Karacolak T, Sekhar PK. (2020). Flexible Antennas: A Review. Micromachine, vol. 11, p. 847. doi: 10.3390/mi11090847.

[2] Al-Haddad MASM, Jamel N, Nordin AN. (2021). Flexible Antenna: A Review of Design, Materials, Fabrication, and Applications. Journal of Physics, vol. 1878, p. 012068. doi: 10.1088/1742-6596/1878/1/012068.

[3] Ruslan AA, Mohamad SY, Malek NFA, Yusoff SH, Ibrahim SN, Isa FNM. (2020). Design of Flexible Microstrip Patch Antenna using Rubber Substrate for Brain Tumor Detection. IEEE Student Conference on Research and Development (SCOReD), pp. 1-5. doi: 10.1109/SCOReD50371.2020.9250994.

[4] Sharma PK, Chung JY. (2023). Evaluation of Polydimethylsiloxane (PDMS) as a Substrate for the Realization of Flexible/Wearable Antennas and Sensors. Micromachines, vol. 14, p. 735. https://doi.org/10.3390/mi14040735

[5] Bakar AA, Hasnan F, Razali AR, Rahim AFA, Osman MS, Ali T, Radzali R. (2019). Polydimethylsiloxane as a Potential Antenna Substrate. Acta Physica Polonica Series A, pp. 938-941. doi: 10.12693/APhysPolA.135.938.

[6] Li J, Jiang Y, Zhao X. (2019). Circularly Polarized Wearable Antenna Based on NinjaFlex-Embedded Conductive Fabric. International Journal of Antennas and Propagation, vol. 2019, pp. 1-8. doi: 10.1155/2019/3059480.

[7] Koohestani M, Azadi-Tinat N, Skrivervik AK. (2023). Compact Slit-Loaded ACS-Fed Monopole Antenna for Bluetooth and UWB Systems With WLAN Band-Stop Capability. IEEE Access, vol. 11, pp. 7540-7550. doi: 10.1109/ACCESS.2023.3238577.

[8] Wearable Antenna for Well-Being. Available: https://bte-jkt.telkomuniversity.ac.id/wearable-antenna-for-well-being-iot-untuk-hidup-yang-lebih-baik/

[9] Kaur H, Chawla P. (2022). Design and Performance Analysis of Wearable Antenna for ISM Band Applications. International Journal of Electronics, vol. 110, pp. 986-1005. doi: 10.1080/00207.2022.2068199.

[10] John AS, Murugan K. (2022). Design and Simulation of a Slotted Inset Feed Patch Antenna for Wireless Body Area Network Applications. International Conference on Knowledge Engineering and Communication Systems (ICKECS), pp. 1-6. doi: 10.1109/ICKECS56523.2022.10060299.

[11] Noor MSNM, Mohamad SY, Malek NFA, Isa FNM, Rahimi AH, Ramli HA. (2024). A Dual-Band Slotted Antenna at 2.4/5.8GHz for ISM Band Applications. IEEE Symposium on Wireless Technology & Application (ISWTA), pp. 67-71. doi: 10.1109/ISWTA62130.2024.10651642.

[12] Ibrahim MS. (2019). Low-Cost, Circularly Polarized and Wideband U-Slot Microstrip Patch Antenna with Parasitic Element for WiGig and WPAN applications. 13th European Conference on Antennas and Propagation (EuCAP), pp. 1-4.

[13] Rahimi AH, Mohamad SY, Malek NFA, Islam MR, Midi NS, Shuhaimi NI. (2024). A Flexible Wideband Microstrip Antenna on TPU Substrate Using Inset Slot Feed and Partial Ground Plane. IEEE Symposium on Wireless Technology & Application (ISWTA), pp. 29-33. doi: 10.1109/ISWTA62130.2024.10651864.

[14] Loss C, Silveira TM, Pinho P, Salvado R, de Carvalho NB. (2020). Design and Analysis of the Reproducibility of Wearable Textile Antennas. 12th International Symposium on Communication Systems, Network and Digital Signal Processing (CSNDSP), pp. 1-5. doi: 10.1109/CSNDSP49049.2020.9249634.

[15] Taqdeer MM, Amjad QM, Zahid M, Amin Y. (2023). 2×2 Hexagonal-Shaped Antenna Array for 5.8 GHz ISM Band Applications. 7th International Multi-Topic ICT Conference (IMTIC), pp. 1-4. doi: 10.1109/IMTIC58887.2023.10178485.

[16] Sawant VG, Kadam P, Mangrulkar V, Gawade H, Patil Y. (2023). 5.8GHz ISM Band Low Cost Button Antenna for Smart Wearable Application. 6th International Conference on Advances in Science and Technology (ICAST), pp. 638-642. doi: 10.1109/ICAST59062.2023.10454967.

[17] Gupta K, Jain K, Singh P. (2021). Analysis and Design of Circular Microstrip Patch Antenna At 5.8 GHz. International Journal of Computer Science and Information Technologies, vol. 5, pp. 3895-3898. doi: 10.1088/1742-6596/1804/1/012200.

[18] Valjibhai GJ, Bhatia D. (2023). Design of 4×1 Microstrip Patch Antenna Array for 5.8 GHz ISM Band Applications. International Conference on Communication and Electronics System Design. *https://doi.org/10.1117/12.2012464.*

[19] Salelkar SS, Kerkar P. (2019). 5.8 GHz Semi Slotted Patch Antennas for ISM Band Applications. International Research Journal of Engineering and Technology (IRJET), vol. 6(4), pp. 3791-3794.

[20] Kumar VR, Anushree T, Aarthi S, Sanju A, Aishwariya VU, Kumar VP. (2021). Design and Analysis of Wearable Textile Jean Antenna for ISM Band Applications. Turkish Online Journal of Qualitative Inquiry (TOJQI), vol. 12(5), pp. 2442-2447.

[21] Saeidi T, Mahmood SN, Alani S, Ali SM, Ismail I, Alhawari ARH. (2020). Triple-Band Transparent Flexible Antenna for ISM Band and 5G Applications. IEEE International Black Sea Conference on Communications and Networking (BlackSeaCom), pp. 1-6. doi: 10.1109/BlackSeaCom48709.2020.9235009.